Influence of Si₃N₄ on Ti-6Al-4V via spark plasma sintering: Microstructure, corrosion and thermal stability

F.M. Kgoete [a, *], A.P.I. Popoola [a], O.S.I. Fayomi [a, b], I.D. Adebiyi [c]

[a] Department of Chemical, Metallurgical & Materials Engineering, Tshwane University of Technology, P.M.B X680, Pretoria, 0001, South Africa
[b] Department of Mechanical Engineering, Covenant University, P.M.B X1034, Ota, Nigeria
[c] Department of Chemical & Metallurgical Engineering, Vaal University of Technology, P.M.B X021, Vanderbijlpark, 1911, South Africa

ABSTRACT

The objective of this research was to study the influence Si₃N₄ on Ti-6Al-4V via spark plasma sintering process. The experiments were performed at a temperature of 1000 °C with a holding time of 6 min under a pressure of 50Mpa.Ti-6Al-4V powder was admixed with different weight proportions of Si₃N₄ powder. Sintered composite samples were produced from the mixture and the influence of Si₃N₄ on the microstructure; mechanical and thermal properties of the composites were investigated. Scanning electron microscope (SEM-EDS) was used to study the bulk morphology of the sintered composites. The phases present in the fabricated sintered composites were observed by energy dispersive X-ray diffraction spectrometer (XRD). Microhardness was investigated by the means of high impact diamond Durascan micros hardness tester. Electrochemical behavior of the sintered samples was measured by potentiodynamic polarization method. The thermal performances of the sintered composites were explored by a Thermal gravimetric analyser (TGA). The experimental results revealed that the microstructure, corrosion resistance and thermal stability properties of the material were improved by the addition of Si₃N₄. The effect of Si₃N₄ on the performance characteristics of Ti6AI4V alloy was seen to be compactable and useful in aerospace application.

© 2018 Elsevier B.V. All rights reserved.

1. Introduction

Excellent mechanical properties of Ti-6Al-4V alloy makes it remain the most widely used material in both biomedical and aerospace applications [1,2]. The main interest for its use derives from its beneficial properties, such as low density, low modulus elasticity, excellent corrosion properties and biocompatibility [3]. However, poor tribological properties (such as high friction coefficient and low hardness [4,5], and corrosion properties (such as, low oxidation resistance) limit the extensive application of Ti alloys in these engineering applications [5,6].

To solve these problems, extensive researches have been embraced to improve the service life of titanium alloys against corrosion, thermal and wear attacks. In recent years, a variety of surface treatment methods have aroused and implemented to improve the existing thermal and mechanical properties of Ti-

alloys. Most of these surface modification processes which includes: Plasma-Enhanced Vapour Deposition Coating, Excimer Laser Surface, Self-Propagating High Temperature Synthesis (SHS) etc. have been developed for improving the thermal, wear, corrosion, hardness properties of this metal [7]. The properties exhibited by the composites fabricated by the techniques establishes further development of the composites for high temperature applications. Amongst the potential solutions, the Powder Metallurgy (PM) process has shown several economic advantages, such as low material wastage and energy consumption. Considerable efforts have been put into titanium powder metallurgy development to improve the inferior properties and Spark Plasma Sintering (SPS) process has been found to be the most important processing technique in that it allows fabrication of bulk materials from powders using a fast heating rate (up to 1000 °C/min) and short holding times at low sintering temperatures lower than most of the conventional sintering techniques [8,20].

Many researchers have investigated on the addition of ceramic particulates to Ti alloys using Spark plasma sintering method and how they affect the mechanical and tribological properties of Ti alloys. The use of titanium nitride (TiN) and titanium boride (TiB) as

ceramic additives has been studied by Dabhade, Rama and Ramakrishnan [9] and Zhang et al. [10] in an attempt to better the microstructural characteristics and mechanical properties of the sintered composites. Lu et al. [11] and Kim et al. [12] explored the use of niobium (Nb) and Hydrogen fluoride (HF) as reinforcement in an attempt to investigate the effect of reinforcements on the high temperature oxidation of Ti based composites. The results showed that the microstructural, mechanical and high temperature oxidation properties of Ti based composites with ceramic additives are improved and various bulk characteristics were obtained depending upon the proportion of the additive. In the current research, an effort has been made to investigate the influence of Si_3N_4 on Ti-6Al-4V through spark plasma sintering focusing on the microstructure, corrosion and thermal stability of resultant composites. Scanning electron microscope attached with energy dispersive spectroscopy (SEM-EDS), X-ray Diffraction (XRD) and thermal gravimetric analyser (TGA) were used for characterization of the composites.

2. Methodology

Titanium powder (Ti-6Al-4V) of (45—90 μm particle spherical, from TLS Technik GmbH) and silicon nitride powder (Si_3N_4) of (−90/+45 μm, 99.9% from Weartech (pty) were blended according to the chemistry proportions, as recorded in Table 1. In order to determine the homogeneity of the materials and to observe the phase formed; scanning electron microscopy attached with energy

Table 1
Starting materials.

Powder	Particle Size (μm)	Density (g/m^3)	Purity
Ti-6Al-4V alloy	45—90	4.43	>99
Silicon Nitride	−90/+45	3.44	>99

dispersive spectroscopy (SEM-EDS) and X-ray Diffraction (XRD) analysis were employed. The powders were then tubular mixed and then consolidated at a temperature of 1000 °C, pressure of 50Mpa, 6 min holding time and a heating rate of 100 °C/min. After Spark plasma sintering process the samples were measured for density using Archimide's principle, and then partitioned into necessary dimensions for microhardness, corrosion, morphology, phases formed and oxidation resistance analysis. Table 1 and Fig. 1 shows the starting materials: Titanium alloy (Ti-6Al-4V) and Silicon Nitride (Si_3N_4) with their particle sizes, densities and purity level.

2.1. Mixing

Ti-6Al-4V and Si_3N_4 powders were tubular mixed at a revolving speed of 50 rpm at room temperature for 4 h. Afterwards, the homogeneity of the tubular mixed powders were analyzed by scanning electron microscopy and the phases formed were analyzed through X-ray diffractometer. The starting powders were weighed in different quantities as presented in Table 2.

2.2. Spark plasma sintering

Spark plasma sintering (SPS FCT Systeme GmbH) model was employed to consolidate the premixed powders that were previously set. Graphite dies of 30 mm diameter and 5 mm thickness were used to load about 30 g of each premixed powder for fabrication. The sintering was done at a temperature of 1000 °C, heating rate of 100 °C/min, and dwelling time of 6 min at a pressure of 50Mpa under argon (Ar) atmosphere.

2.3. Densification studies

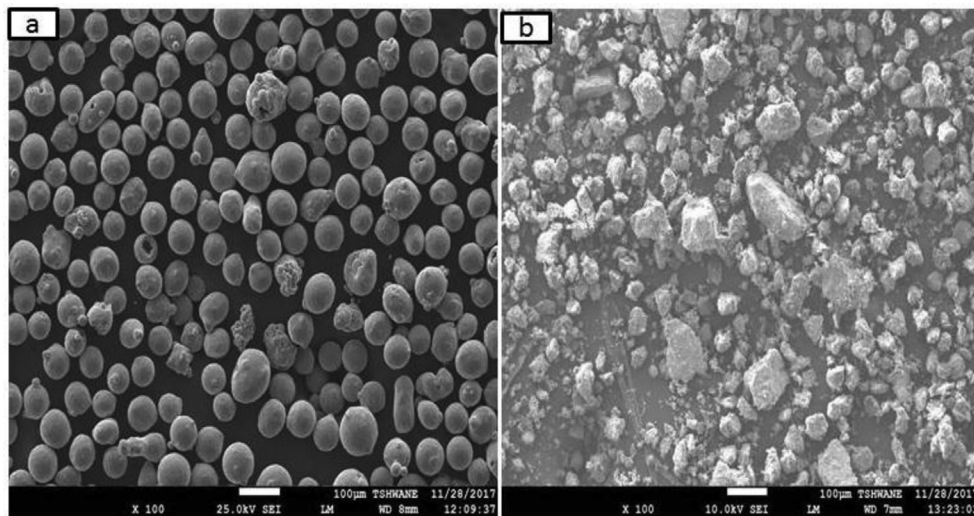To explore the impact of Si_3N_4 particulates on Ti-6Al-4V alloy,

Fig. 1. SEM photographs of starting materials. a) Ti-6Al-4V and b) Si_3N_4.

Table 2
Properties of sintered Ti-6Al-4V and Ti-6Al-4V-Si_3N_4 composites at 1000 °C.

Sample	Measured density (cm^3)	Theoretical density (g/m3)	Relative density (%)	Porosity (%)	Sintering temperature (ºC)
Ti-6Al-4V	4.369586	4.43	98.6	1.4	1000
Ti-6Al-4V-5Si_3N_4	4.231772	4.367	96.9	3.1	1000
Ti-6Al-4V-10Si_3N_4	4.187542	4.306	97.2	2.8	1000
Ti-6Al-4V-15Si_3N_4	4.090138	4.25	96.2	3.8	1000

density measurements were done using Archimedes' principle. This principle was employed to determine the densities of the sintered compacts with deionized water as the immersion liquid and in air. The densitometer automatically calculated the density of each compact using Archimedes' principle. The recorded density was an average of five measurements carried out on each sample and the relative density was subsequently calculated as a function of both the theoretical and measured density of the sintered composites [13].

2.4. Microhardness studies

Spark plasma sintered Ti-6Al-4V and Ti-6Al-4V-Si$_3$N$_4$ composites specimen were evaluated for microhardness by the use of Emco microhardness tester with a dura scan diamond indenter. Indentations were made across the sintered surface at three locations using a load of 10 g for 10sec and the average hardness was used as a final microhardness of the materials.

2.5. Electrochemical studies

A conventional three electrode cell, consisting of saturated calomel (SCE), graphite, and spark plasma sintered sample as reference, auxiliary, and working electrode respectively, was used to study the electrochemical behavior of sintered Ti-6Al-4V and developed Ti-6Al-4V-xSi$_3$N$_4$ in 3.65 wt. % NaCl +0.1 M HCl solution. Working electrode was exposed to the solution. The electrochemical measurement was done with Autolab PGSTAT 101 potentiostat. The potentiodynamic potential scan was fixed to run from −1.5 V to +1.5 mV with scan rate of 0.012 V. The relationship is in line with the standard mentioned by Fayomi et al. [14].

2.6. Thermal oxidation studies

Thermal Gravimetric Analyser was employed for the measurement of oxidation resistance of the sintered composites. The TGA machine consists of a sample pan that is supported by a precision balance and a purge gas. The pan resides in a furnace and it is heated and cooled during the experiment while a sample purge gas is responsible for controlling the sample environment. During experiment, the mass of the substance is monitored as a function of temperature or time as the sample specimen is subjected to a controlled temperature program in a controlled atmosphere. The composites were studies at a temperature of 45 °C to 800 °C at a heating rate of 10 °C/min in an oxygen atmosphere.

3. Results and discussion

3.1. Starting powders and morphological studies

Fig. 1(a) and (b) show the SEM morphology of Ti-6Al-4V and Si$_3$N$_4$ powders respectively. Ti-6Al-4V powders are spherical, not porous and there is no evidence of agglomeration in the particles [15]. It could be seen that the size distribution of the silicon nitride powder in Fig. 1(b) is uneven and the shape is hexagonal. Fig. 2(a−d) shows the scanning electron microscopy (SEM) images of Ti-6Al-4V with and without Si$_3$N$_4$ powders. It could be seen that the scanning electron microscopy reveals a reasonably uniform distribution of Si$_3$N$_4$ in the Ti-6Al-4V alloy matrix and no pores are observed in the developed composites. The microstructural evolution of the composites was related to various proportions of Si$_3$N$_4$ added. The microstructures of Ti-6Al-4V with varying Si$_3$N$_4$ fractions do not reveal any presence of pores; this may be attributed to the morphology of the starting materials and affirmed by the high densification percentage achieved on the composites. Falodun et al.

[16]; tubular mixed of Ti-6Al-4V with nanosized TiN powder and achieved even distribution of TiN within the titanium alloy powder. This microstructural observation indicates that there is an interaction between Si$_3$N$_4$ particles and Ti-6Al-4V alloy during the spark plasma sintering processing. As illustrated in Fig. 2(a−d), the microstructures reveal that, some Si$_3$N$_4$ particulates diffuses into the interface of Ti-6Al-4V grains.

3.2. XRD analysis

Fig. 3 shows the diffraction patterns of Ti-6Al-4V with and without Si$_3$N$_4$ at the sintering temperature of 1000 °C and holding time of 6 min. The XRD patterns of the sintered composites reveal prevalence of diffraction peaks corresponding to the metallic material used in the study. The presence of titanium, aluminum and Silicon nitride peaks can be observed with silicon nitride and aluminum being characterized by low intensities of diffraction peaks. However, vanadium peaks could not be firmly established. This may be attributed to the small amount of vanadium making it undetectable. Zhang and Kobayashi [17] indicated that due to small relative amount of CZTS (Cu$_2$ZnSnS$_4$), the XRD was unable to detect secondary phases. Employing XPS analysis revealed peaks of secondary phases owing to the analysis being a highly sensitive analysis to chemical states. This indicates that XPS can be used to detect small amounts of chemicals and phases that are undetectable in XRD.

3.3. Relative density and microhardness properties

The relative densities of the compacts alloy can be observed in Fig. 4. In general it is noticed that the relative densities of the spark plasma sintered Ti-6Al-4V reinforced with Si$_3$N$_4$ decreases with Si$_3$N$_4$ addition. Falodun et al. [12] obtained a decrease in relative density with increasing nano-sized TiN addition. It can generally be said that the addition of ceramic reinforcement to Ti-6Al-4V alloy decreases the relative density of the alloy however the decrease in relative density does not affect the mechanical, electrochemical and thermal properties of the composites (See Figs. 5−7).

Fig. 5 illustrates the effect of weight percentage (Si$_3$N$_4$ wt.%) of silicon nitride on hardness property of Ti-6Al-4V alloy. From the observed hardness values in Fig. 5, it can be described that silicon nitride powder addition on Ti-6Al-4V significantly improves the hardness properties of the developed spark plasma sintered Ti-6Al-4V-based composite. This may be attributed to the fact that Si$_3$N$_4$ is the most thermodynamically stable ceramic material and it exhibits high hardness values than most metallic materials. There is a drastic improvement of hardness property of the developed spark plasma sintered compacts reinforced with Si$_3$N$_4$.

3.4. Electrochemical studies

Corrosion properties of spark plasma sintered (SPS) Ti-6Al-4V-Si$_3$N$_4$ were investigated in 3.65NaCl containing 0.1 M HCl environments with the aid of potentiodynamic polarization technique. The polarization resistance of the developed compacts is shown in Table 3 and Fig. 6. With reference to Table 3 it was observed that Ti-6Al-4V-10Si$_3$N$_4$ had 8976Ω. With reference to Figs. 4 and 5, Ti-6Al-4V-10Si$_3$N$_4$ showed improved hardness property with a higher relative density as compared to the other reinforced composites. Hence it was expected that Ti-6Al-4V-10Si$_3$N$_4$ possess the most corrosion resistance properties with the least corrosion rate. The corrosion rate of 0.030547 mm/yr was achieved. Furthermore, the developed sintered composites showed to possess better corrosion resistance properties with Si$_3$N$_4$ addition in this order Ti-6Al-4V, Ti-6Al-4V-5Si$_3$N$_4$, Ti-6Al-4V-15Si$_3$N$_4$, and Ti-6Al-4V-10Si$_3$N$_4$. It can be
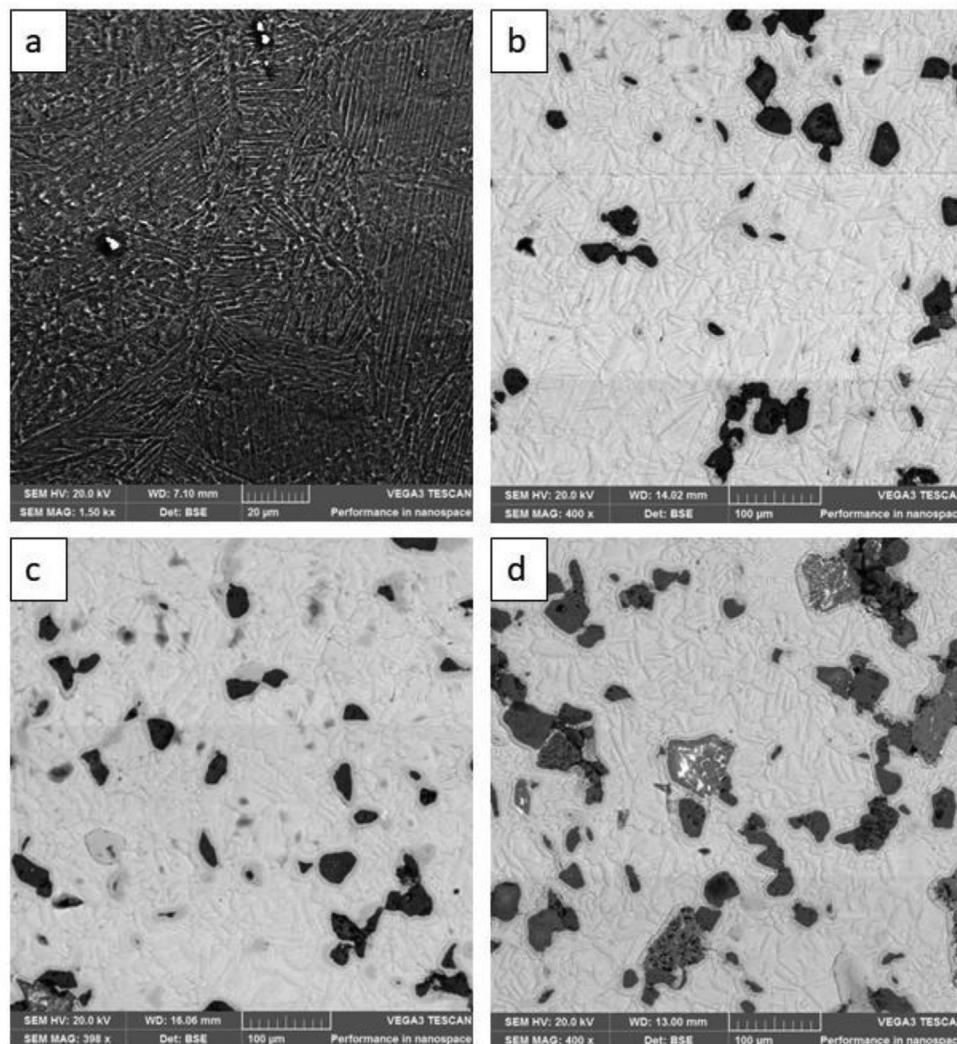
Fig. 2. SEM images of a) Ti-6Al-4V, (b) Ti-6Al-4V-5Si$_3$N$_4$, (c) Ti6Al4V-10Si$_3$N$_4$, and (d) Ti-6Al-4V-15Si$_3$N$_4$.

concluded that the addition of Si$_3$N$_4$ on the Ti-6Al-4V significantly improves the corrosion resistance properties.

3.5. Thermal oxidation studies

The high temperature oxidation resistance of Ti-6Al-4V and Ti-6Al-4V-Si$_3$N$_4$ composites have been evaluated by thermal gravimetric analyser (TGA). Weight change of the composites due to oxidation from 45 to 800 °C is presented in Fig. 7. The onset temperature of Ti-6Al-4V is about 650 °C where there is a rapid drop in mass which indicates high temperature instability. It can be seen that the weight loss of Ti-6Al-4V-10Si$_3$N$_4$ composites is much lower than that of Ti-6Al-4V alloy, displaying a significant improvement of the high temperature oxidation resistance. This might be attributed to the adhesion of Si$_3$N$_4$ powder between the oxide scale and the alloy as well as the reduction of the oxide growth rate by silicon nitride atoms through blocking of diffusion paths. Fig. 8 displays the morphology of the oxide layers on the surface obtained at temperatures of 45°C-800 °C.

Fig. 8 (a) reveals the morphology of thermally oxidized Ti-6Al-4V at temperatures of 45−800 °C for 95 min. The morphology shows the presence of a uniform oxide layer which evenly covered the examined surface of the sample with signs of porosity. Guleryuz

and Cimenoglu [18], indicated that the high affinity of titanium to oxygen results in the formation of very thin oxygen layer on the surface. Rutile and anatase are the most common modifications of TiO$_2$ that forms as an oxide layer. However, at temperatures above 400 °C, a thick oxide layer (OL) forms. This TiO$_2$ scale is poorly adherent, defective and brittle, hence the Ti and O ions can easily diffuse through the porous oxide leading to fast oxidation kinetics [18]. Observing Fig. 8 (a) a thick oxide scale can be observed. This feature confirms the poor high temperature oxidation of the Ti-6Al-4V alloy [19].

Fig. 8(b) displays the morphology of Ti6Al4V alloy reinforced with silicon nitride. Tegner et al. [20], indicated that oxidation resistance of Ti6Al4V alloy at high temperatures can be improved by addition of silicon. Silicon causes the formation of a thin SiO$_2$-layer at the metal oxide interface forming a diffusion barrier for oxygen. Guleryuz and Cimenoglu [18] mentioned that the ultimate goal of thermal oxidation is to create a relatively thin, mechanically stable oxide layer that can bring about remarkable protection against friction and wear. Observing Fig. 8(b) a relatively thin oxide layer can be observed this may be attributed to silicon which has been known to causes formation of a thin SiO$_2$-layer at the metal oxide interface forming a diffusion barrier for oxygen.
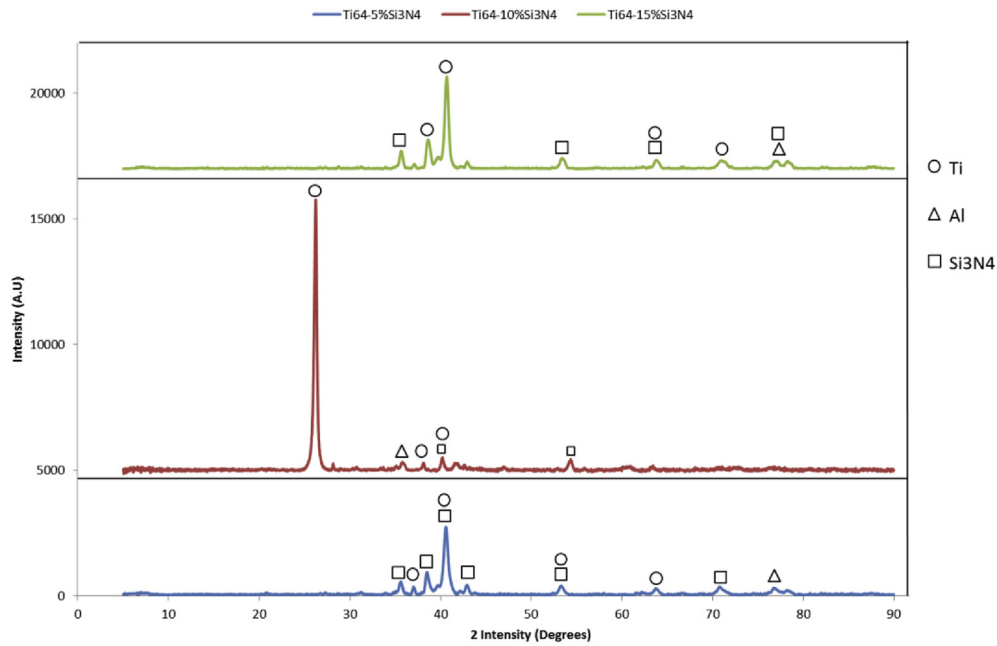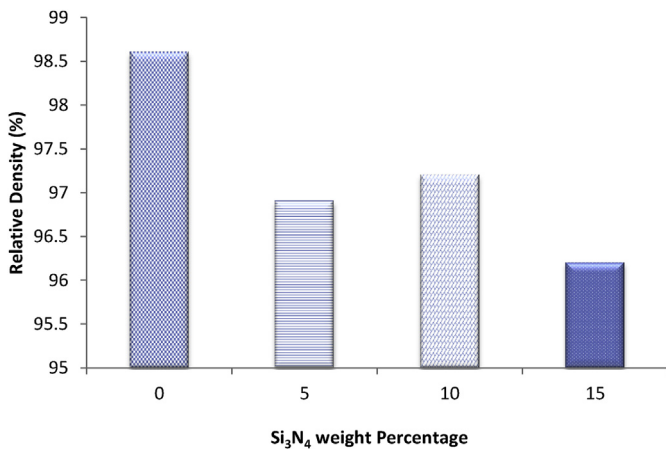
Fig. 3. XRD diffractogram of Ti-6Al-4V-Si$_3$N$_4$.

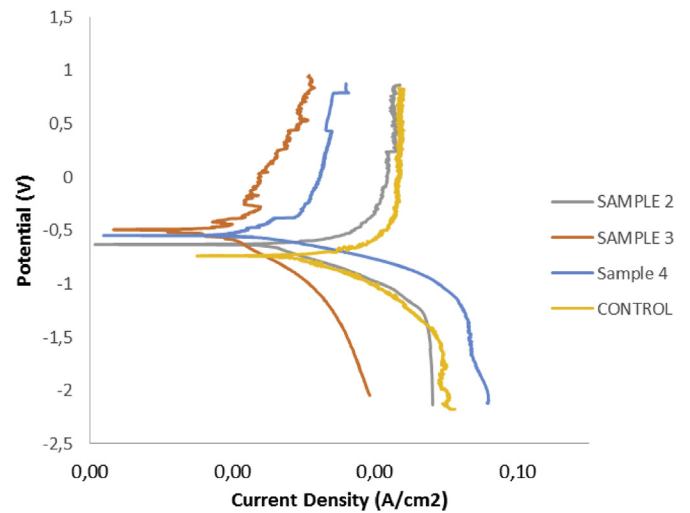**Fig. 4.** Relative densities of the sintered compacts of Ti-6Al-4V and developed Ti-6Al-4V-Si$_3$N$_4$.

Fig. 6. Potentiodynamic polarization curves for Ti-6Al-4V (Control), Ti-6Al-4V-5Si$_3$N$_4$ (sample 2), Ti-6Al-4V-10Si$_3$N$_4$ (Sample 3) and Ti-6Al-4V-15Si$_3$N$_4$ (Sample 4).
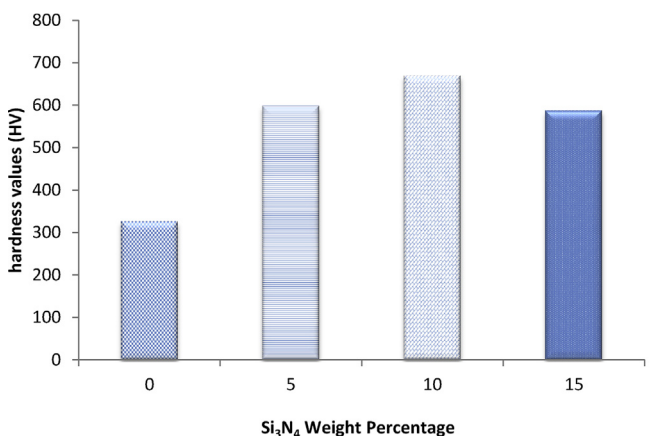
4. Conclusion

Spark plasma sintering method was effectively applied for fabrication of three composites reinforced with various additions of micron-sized silicon nitride content and the influence of this reinforcement particulate on the densification behavior, micro-structure, corrosion and thermal stability properties was explored. The following conclusions can be made from the discussions are as follows.

1. Reported result shows that addition of silicon nitride to Ti-6Al-4V alloy have critical impact on densification, hardness, micro-structure, corrosion and thermal stability of the sintered compacts.
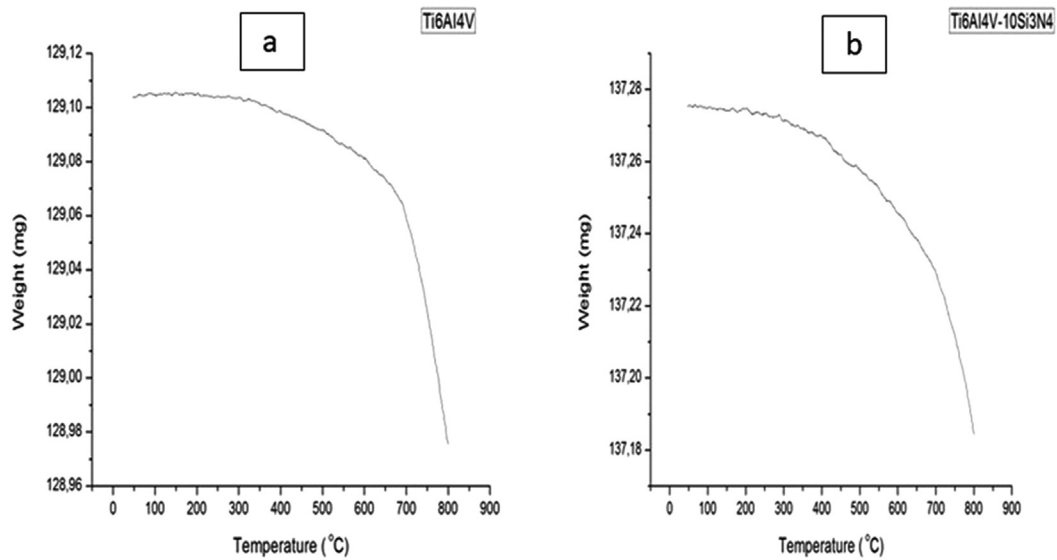

Fig. 5. Hardness properties of Ti-6Al-4V and Ti-6Al-4V-Si$_3$N$_4$ sintered composites.

Fig. 7. Thermal oxidation graphs of a) Ti-6Al-4V, and b) Ti-6Al-4V-10Si$_3$N$_4$.

Table 3
Linear polarization tafel data.

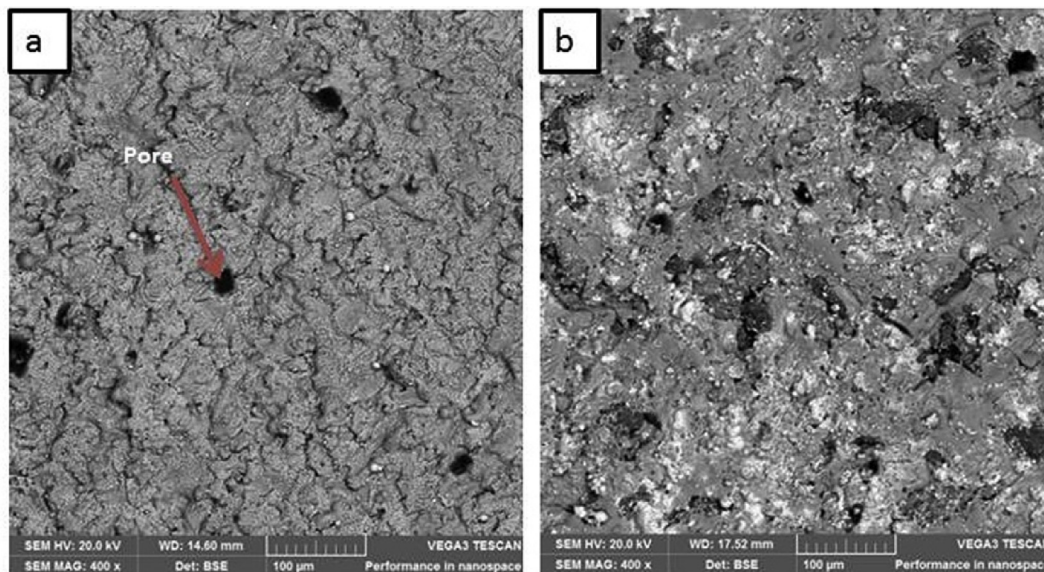| Sample	E_{corr}(V)	j_{corr} (A/cm^2)	Corrosion rate (mm/year)	Polarization resistance (Ω)
Ti-6Al-4V	−0,9463	3,17E-07	0.986625	989
Ti-6Al-4V-5Si$_3$N$_4$	−0,53232	0,00003098	0.08234	7654
Ti-6Al-4V-10Si$_3$N$_4$	−0,49506	3,94E-05	0.030547	8976
Ti-6Al-4V-15Si$_3$N$_4$	−0,50098	3,67E-05	0.0671	8290

Fig. 8. SEM images of a) Ti-6Al-4V and b) Ti-6Al-4V-Si$_3$N$_4$.

2. Tubular mixing of Ti-6Al-4V with micron-sized silicon nitride powder resulted in a fine dispersion within the titanium alloy powder.
3. The hardness of the sintered composites significantly improved upon reinforcing Si$_3$N$_4$ to Ti-6Al-4V alloy powder.
4. Ti-6Al-4V reinforcement by Si$_3$N$_4$ particulates improves hardness and the corrosion-resistance properties of Ti-6Al-4V in 3.65%NaCl +0.1 M HCl environment.

5. The oxidation testing of spark plasma sintered Ti6Al4V alloy shows that the addition of Si$_3$N$_4$ can effectively improve the oxidation resistance of the alloy at 800 °C in air.

Acknowledgements

References

[1] G.D. Revankar, R. Shetty, S.S. Rao, V.N. Gaitonde, Wear resistance of titanium alloy (Ti-6Al-4V) by ball burnishing process, J. Mater. Research Technol. 6 (1) (2017) 13—32.

[2] A.O. Adegbenjo, E. Nsiah-Baafi, M.B. Shongwe, P.A. Olubambi, J.H. Potgieter, Low temperature spark plasma sintered irregular shaped Ti-6Al-4V powders with enhanced properties, J. Eng. Technol. 6 (1) (2017) 35—48.

[3] R.S. Razavi, M. Salehi, M. Ramazani, H.C. Man, Corrosion behavior of laser gas nitride Ti-6Al-4V in HCl solution, J. Corros. Sci. 51 (10) (2009), 2334-2329.

[4] L. Xiao, S. Tian, X. Bao, L. Chen, Creep properties and effect factors of hot continuous rolled Ti6Al4V alloy, Mater. Sci. Eng., A 529 (2011) 452—458.

[5] J.H. Luan, Z.B. Jiao, G. Chen, C.T. Liu, Improved ductility and oxidation resistance of cast Ti-6Al-4V alloys by microalloying, J. Alloys Compd. 602 (2014) 235—240.

[6] R. Gaddam, B. Sefer, R. Pedesson, M.L. Antti, Study of alpha-case depth in Ti-6Al-2Sn-4Zr-2M0 and Ti-6Al-4V, Mater. Sci. Eng. 48 (2013) 2—9.

[7] V. Vijay, K. Arjun, A. Kumar, A.V. Kumar, P. Chandrasekar, V. Balusamy, Review of various surface treatment techniques on titanium alloys and their protective effects against corrosion, J. Surf. Sci. Technol. 23 (2007) 49—58.

[8] A. Lisiecki, J. Piwnik, Tribological characteristics of titanium alloy surface layers produced by diode laser gas nitriding, Arch. Metall. Mater. 61 (2) (2016) 543—552.

[9] V.V. Dabhade, T.R.M. Mohan, P. Ramakrishnan, Sintering behavior of titanium-titanium nitride nanocomposite powders, J. Alloys Compd. 453 (2008) 215—221.

[10] Z. Zhang, X. Shen, F. Wang, S. Wei, S. Li, H. Cai, Microstructure characteristics and mechanical properties of TiB/Ti-1.5Fe-2.25Mo composite synthesized in situ using SPS process, Trans. Nonferrous Met. China 23 (2013) 2598—2604.

[11] X. Lu, X.B. He, B. Zhang, X.H. Qu, L. Zhang, Z.X. Guo, J.J. Tian, High-temperature oxidation behavior of TiAl-based alloys fabricated by spark plasma sintering, J. Alloys Compd. 478 (2009) 220—225.

[12] K.M. Kim, J.T. Yeom, H. Lee, S. Yoon, J.H. Kim, High temperature oxidation behavior of Ti-Ni-Hf shape memory alloy, Thermochim. Acta 583 (2014) 1—7.

[13] K. Machethe, A.P.I. Popoola, S. Aigbodion, O.M. Popoola, Electrochemical study of spark plasma-sintered copper reinforced with Ni/SiC micron-size particles for electrical applications, Iran. J. Sci. Technol. Trans. A-Science (2017) 1—8.

[14] O.S.I. Fayomi, M. Abdulwahab, A.P.I. Popoola, Properties evaluation of ternary surfactant-induced Zn-Ni-Al2O3 films on mild steel by electrolytic chemical deposition, J. Ovonic Research 9 (5) (2013) 123—132.

[15] A.O. Adegbenjo, A. Nsiah-Baafi, M.B. Shongwe, M. Ramakokovhu, P.A. Olubambi, Dependence of densification, hardness and wear behaviors of Ti6Al4V powders on sintering temperature, Int. J. Chem., Mol., Nucl., Mater. Metall. Eng. 10 (2016) 560—566.

[16] O.E. Falodun, B.A. Obadele, S.R. Oke, M.O. Maja, P.A. Olubambi, Effect of sintering parameters on densification and microstructural evolution on nano-sized titanium nitride reinforced titanium alloys, J. Alloys Compd. 736 (2018) 202—210.

[17] X.F. Zhang, M. Kobayashi, Identification of Secondary Phases in Cu2ZnSnS4 Layers by In-depth Resolved X-ray Photoelectron Spectroscopy Analysis, International Center for Science and Engineering Programs, 2017, pp. 1—8.

[18] H. Guleryuz, H. Cimenoglu, Oxidation of Ti-6Al-4V alloy, J. Alloys Compd. 472 (2009) 241—246.

[19] C. Huang, Y. Zhang, J. Shen, R. Vilar, Thermal stability and oxidation resistance of laser clad TiVCrAlSi coatings on Ti-6Al-4V alloy, Surf. Coating. Technol. 206 (2011) 1389—1395.

[20] B.E. Tegner, L. Zhu, C. Siemers, K. Saksl, G.J. Ackland, High temperature oxidation resistance in titanium-niobium alloy, J. Alloys Compd. 643 (2015) 100—105.